Light Attenuation Display: Subtractive See-Through Near-Eye Display via Spatial Color Filtering

Yuta Itoh, Tobias Langlotz, Daisuke Iwai, Kiyoshi Kiyokawa, and Toshiyuki Amano

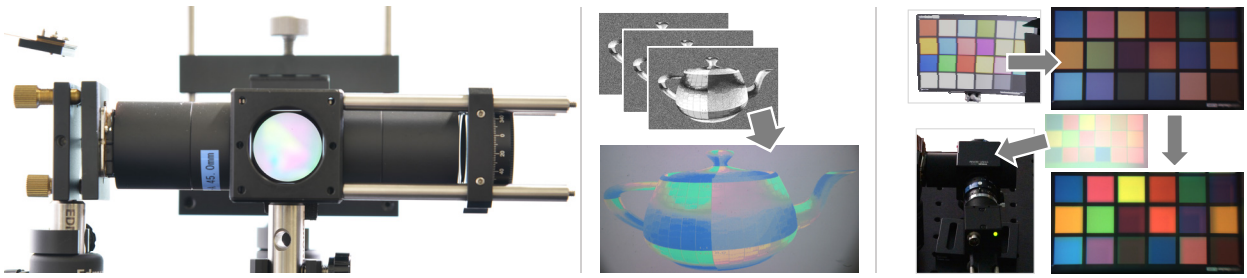

Fig. 1. The light attenuation display. (Left) Our prototype of a light attenuation display positioned close to the user-perspective camera's viewing point. (Middle) An example image created with our light attenuation display; the successive gray-scale images are input phase images and the bottom image is a real color image captured by a user-perspective camera. (Right) Example application of enhancing the real-world view by using the system. The view of a colored checkerboard is augmented by alignment of our spatial color filter with the scene, which results in an augmented view of the same colored checkerboard but with a more vivid appearance. Note that the two images are captured under the same illumination with the same capture settings, including exposure time, gamma, and white balance.

Abstract— We present a display for optical see-through near-eye displays based on light attenuation, a new paradigm that forms images by spatially subtracting colors of light. Existing optical see-through head-mounted displays (OST-HMDs) form virtual images in an additive manner—they optically combine the light from an embedded light source such as a microdisplay into the users' field of view (FoV). Instead, our light attenuation display filters the color of the real background light pixel-wise in the users' see-through view, resulting in an image as a spatial color filter. Our image formation is complementary to existing light-additive OST-HMDs. The core optical component in our system is a phase-only spatial light modulator (PSLM), a liquid crystal module that can control the phase of the light in each pixel. By combining PSLMs with polarization optics, our system realizes a spatially programmable color filter. In this paper, we introduce our optics design, evaluate the spatial color filter, consider applications including image rendering and FoV color control, and discuss the limitations of the current prototype.

Index Terms—Light attenuation display, phase modulation, see-through display, vision augmentation, augmented reality

1 Introduction

Optical-see through head-mounted displays (OST-HMDs) integrate an image into the user's view to augment the appearance of the real world as perceived by the user. However, OST-HMDs only *add* light: the displayed image is blended with the background using an optical combiner. Many of the fundamental issues with OST-HMDs result from this light-additive principle. For example, OST-HMDs are problematic in bright environments because the display must be bright enough to add extra light that can be perceived in front of the bright background [34]. Similarly, no commercially available OST-HMDs can intentionally make a real scene darker or display dark colors when the environment is bright. While some researchers have used LCDs to selectively block out individual pixels in OST-HMDs (e.g., for creating the effect of occlusions) [19], there have been no attempts to build systems using a per pixel color filter to implement such a head-mounted display.

In this work, we propose a light attenuation display technique that enables a completely different category of OST-HMDs. Instead of adding light, light attenuation displays provide additional visual information by subtracting light from the physical environment using dynamic per-pixel color filters. Displays utilizing this concept do not need their own background light; instead, they use light from the environment. The middle panel of Figure 1 shows a basic example of a light attenuation display by selectively filtering white light emitted from the physical environment to display an image. The advantages of this approach become apparent when again considering that existing OST-HMDs (e.g., Microsoft's Hololens) usually integrate optical shades to darken the environment, consequently improving the contrast of the digital overlay in bright environments. Our proposed technique would perform best in the conditions with which existing OST-HMDs struggle the most, such as bright outdoor environments.

While there are different avenues for implementing the concept of light attenuation displays, the core components of our implementation are phase-only spatial light modulators (PSLM [6, 25, 40]), typically made from a liquid crystal (LC) material. Using an electrically controlled birefringence effect, PSLMs can control the delay of light (i.e., phase shift or retardance). In this work, we show how this effect can be used to build a prototype for a light attenuation display that is characterized by better light efficiency compared to other possible implementations (e.g., a transmissive LCD panel).

In addition to being able to filter incoming light on a per-pixel level to change the appearance of the environment or to display digital information, the ability to combine both per-pixel color filtering and per-pixel color blending, as in existing OST-HMDs, is promising. This would allow many applications that are currently not possible as it would provide full control of the light within a head-mounted display.

- *Yuta Itoh is with Tokyo Institute of Technology.*
- *Tobias Langlotz is with University of Otago.*
- *Daisuke Iwai is with Osaka University.*
- *Kiyoshi Kiyokawa is with Nara Institute of Science and Technology.*
- *Toshiyuki Amano is with Wakayama University.*

Manuscript received 10 Sept. 2018; accepted 7 Feb. 2019.
Date of publication 17 Feb. 2019; date of current version 27 Mar. 2019.
For information on obtaining reprints of this article, please send e-mail to: reprints@ieee.org, and reference the Digital Object Identifier below.
Digital Object Identifier no. 10.1109/TVCG.2019.2899229

Table 1. Comparison of the basic features of conventional OST-HMDs and our light attenuation display. The two systems have various complementary features.

	OST-HMDs	Our system
Image formation mechanism	additive	subtractive
Image illumination	active	passive
Brightness limited by	display	environment
Color range	RGB	multispectral
Visibility under luminous scene	low	high
Visibility under dark environment	high	low

Fig. 2. Comparison of ordinary OST-HMDs and our light attenuation display. OST-HMDs form images by adding light from internal illumination. Our system modulates the color of the background light. See also Table 1 for a qualitative comparison.

This complete color control typically requires a hardware design such as video-see through HMDs, where the physical environment is fully mediated by the camera, but with our proposed technique, it would be possible with a see-through design. Similarly, full control of incoming light and ability to add light would also allow high-dynamic-range OST-HMDs. This conceptual high-dynamic-range OST-HMD design would also go beyond existing approaches that increase the dynamic range by using an LCD panel [7] or by trying to compensate the color in software [23] as we can now filter not only the overall intensity but also individual colors on a per pixel basis.

Overall, this paper proposes the idea of near-eye light attenuation displays via spatial color filtering together, explores a prototypical implementation, and discusses limitations and applications of the concept. The proposed concept is in many ways the exact opposite of existing OST-HMDs, and it shines in particular where current solutions have issues and vice versa (see Table 1 and Fig. 2). Our main contributions can be summarized as follows:

- A novel hardware design for see-through head-mounted displays that relies on filtering light from the environment rather than adding light to the scene and as such forms images in a complementary way against ordinary optical see-through displays.
- An implementation of subtractive see-through head-mounted displays using spatial color filtering based on a phase-only spatial light modulator.
- Demonstration of the feasibility of the proposed approach, including results from first experiments and discussion of possible applications.

2 Related Work

In the following, we give an overview of approaches related to our work. We particularly emphasize existing works on head-mounted display technologies and LCD projectors as they share many commonalities with our concept, but we also introduce works on color filters as used in other optical systems.

2.1 Head-Mounted Displays with Spatial Light Modulators

The first HMDs utilized cathode ray tube (CRT) screens to add information to a scene [33], but recently, reflective liquid crystal on silicon (LCOS) panels have become a common display technology used in OST-HMDs. A reflective LCOS is an SLM that can modulate the amplitude of incoming polarized light. Combined with polarized RGB light sources such as LEDs with a polarizer, a reflective LCOS can form an image via amplitude modulation. This implementation essentially needs independent light sources that cover all three RGB color channels. Commodity VR HMDs directly use color LCD panels by combining focal optics so that the user can focus on images of the display placed closer to the eyes.

In OST-HMDs, SLMs are a common tool to realize mutual occlusion [9]. Kiyokawa et al. [21] developed an occlusion-capable OST-HMD in which they use an LCD as a shadow mask to block incoming background light rays. They later upgraded their optics design to maintain the user's viewpoint unchanged by using relay optics [20]. Other occlusion designs use reflective SLMs such as LCoS [3, 10, 11]. Compared to the above transmissive design, these works realize more compact form factors. Other works propose more sophisticated transmissive designs. Yamaguchi et al. [39] combined microlens plates with a transmissive LCD to realize multi-viewpoint occlusion. Maimone et al. [27] used multistack LCDs to configure light-field OST-HMDs together with optical occlusions. Their implementation causes occlusion masks appear dull since the LCD for occlusion is too close to the eyes to be accommodated by a user. Itoh et al citeitoh2017occlusion proposed a compensation method for such occlusion by displaying a compensation image, which is generated by a scene camera, on an OST-HMD.

Some approaches for displays, even head-mounted displays, use PSLMs. Historically, PSLMs have been used in computational holograms to form images. This direction of research led to the application by some works of PSLMs to HMDs. Maimone et al., for instance, proposed a see-through holographic display using a PSLM [28]. Their idea is based on the use of a PSLM in digital holography. Their system uses RGB laser sources and displays time-multiplexed phase patterns on a PSLM so that each laser beam forms a holographic image via the created interference pattern.

Matsuda et al. proposed a focal surface display that uses a PSLM for accommodation modulation [30]. They used a PSLM as a dynamic free-form lens. Their system inserts a PSLM in the optical path of conventional VR HMD optics; then the system modulates the phase of the PSLM based on the depth of the scene to be rendered. Their solution enables a display that allows focus accommodation.

Inspired by those see-through optics designs, we configure our attenuation display with polarized optics to enable both see-through and color interference capabilities. Our work is closely related to the reflectance display proposed by Glasner et al. [12]. They use a PSLM as a spatial reflectance modulator that can display reflectance functions. While their system is unique regarding the display of reflectance functions, it does not aim to display multispectral images and is not a see-through system, which is the focus of our system.

2.2 Projectors

Projectors are devices commonly used in AR to modulate the appearance of the real world [13]. A traditional projector typically uses transmissive LCDs. These LCDs in projectors work as amplitude modulators that reduce the amount of light passing through them. Unlike our system, such modulations do not filter colors and require colored light input. A triple LCD projector splits white light via dichroic mirrors and beamsplitters into each color channel; then, each color of light reaches the dichroic prism, which merges the split light back into a single beam. Such projectors attach three LCDs around the three sides of the prism, allowing the LCDs to modulate the light of each color channel simultaneously.

A single digital mirror device (DMD) projector design only has a DMD as a reflective SLM; thus, it combines a color wheel that can modify the color of the white light from the internal light source. By modulating the DMD synchronously with the spinning color wheel, such projectors can form RGB images. However, this design causes time breaking and loses roughly 2/3 of the original light due to the color filter.

Damberg et al. proposed a high-dynamic-range (HDR) projector system that incorporates a PSLM [7]. Their LCD projector places an extra PSLM between the path of the light from the light source and the LCDs. The PSLM optimizes the direction of light rays so that they cover brighter image areas more than darker image areas.

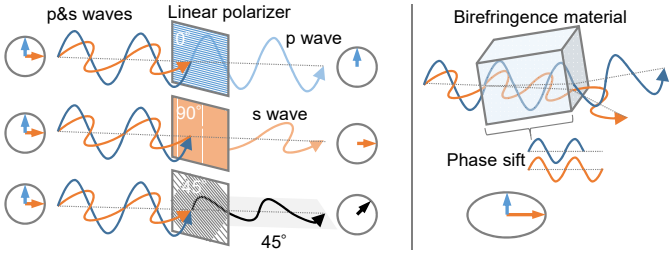

Fig. 3. Schematic explanation of polarization and birefringence. (Left) S- and P-wave light passes through a linear polarizer. Depending on the angle of the linear polarizer, only the s or the p wave is observed on the other side of the polarizer. If the angle of the polarizer is set to 45°, 45°-polarized light comes out, which is inherited from both the p and the s waves. (Right) Light consisting of p and s waves passes through a birefringence material. Due to their refractance differences along specific axes inside the material, the two waves gives phase differences, which results in the light exiting the material in a different direction.

2.3 Color Filter Displays and Multispectral Cameras.

Color filters are commonly used in photography, particularly for monochrome black and white photography. Unlike static color filters, LC tunable color filters can dynamically control their band-pass wavelength, allowing cameras to capture hyper-spectral images. This mechanism is closely related to our system, yet such color filters do not have a pixel structure and thus can only control the color over the entire image.

Post et al. proposed a subtractive color display that combines a multispectral light source from a metal halide lamp with cascaded polarizers and LCD panels [31]. They developed custom color polarizers that mostly work as color filters. However, they are fixed in color channels, unlike our dynamic system.

The work by Wetzstein et al. is the closest to ours [38]. Their proof-of-concept prototypes are based on an LCD panel as used in projectors or a color thin-film transistor (TFT) active-matrix LCD with RGB filters. While Wetzstein et al.'s prototype does not yet have an HMD form factor, they show applications similar to those we demonstrate. Our design stands out as we are the first to demonstrate the use of PSLMs for this specific purpose. Our design has advantages, including more complex color band properties not limited to RGB. In addition, their system is severely affected by the amount of light transmitted to the eye as it only transmits 10% of the incoming light due to the Bayer filter [2]. Our reflective design currently maintains around 20% transmittance depending on the chosen color bands, which is comparable to bright sunglasses.

Consequently, the quality of the images in our results is higher than the results demonstrated by Wetzstein et al. Their work mainly focuses on filtering the amount of light (e.g., adapting the contrast with the environment) and not on filtering individual frequencies. Instead, our demonstrated concept is capable of producing an actual colored image by filtering incoming light or enhancing the colors of the physical environment using frequency modulation.

Multispectral or hyperspectral cameras commonly use narrow-band color filters to pass selected primary colors [29] or diffraction gratings to split incoming light into a continuous color spectrum [4]. The sensors of conventional RGB color cameras are coated with RGB color filters on each pixel [2], which results in a mosaic pattern of RGB filters known as the Bayer pattern. Some commercial multispectral cameras extend the idea by mounting prism gratings directly on their CMOS sensors to assign different spectral bands to each segment of the sensor.

Some existing works use PSLMs for color control. Harm et al. used a PSLM in combination with white illumination to realize a color projector without color masks [15]. Their work is based on the same physical phenomena we use, yet their optics design is not see-through and does not consider adaptive modulation of the filter color. Thai et al. used a PSLM for a color polarization imager that can capture the color and the polarization state of the scene light [35]. Kozacki et al. developed a color holographic display using a PSLM as a color filter, but their system uses LED light sources for dedicated RGB colors [22]. Wang et al. recently demonstrated megapixel adaptive optics with a PSLM to correct the optical aberration of camera views to regain sharp images [36].

Overall, to the best of our knowledge, only a few works have demonstrated subtraction-based display systems, and none specifically aims to realize applications in augmented reality (AR) and augmented vision, such as color management.

3 Polarization-based Colour Filters

Our prototype for a light attenuation display uses the idea of pixel-level color filters. Our specific implementation uses polarization optics [16] to achieve this. To introduce the readers to the mechanism of PSLM-based color filters, we first briefly review two essential optics properties, *polarization* and *birefringence*, which are important phenomena in manipulation of color via phase modulation. We then further introduce the core mathematical tool in polarization optics, so-called Jones calculus, which bridges the phase modulation and color filtering in the polarized optics.

3.1 Polarization and Birefringence

From a physical point of view, light consists of electromagnetic waves vibrating in random directions. When such vibrations are limited to one specific direction or limited in a particular way, the light is called polarized. We can control the polarization state of light by using specific materials such as crystals as well as filters designed to control polarization, which are commonly called polarizers.

Figure 3, top left, illustrates the effect of a linear polarizer, which only passes incident light corresponding to its polarization angle. When light consisting of both p- and s-polarized light (i.e., light parallel or vertical to the incident angle of a given linear polarizer) enters a linear polarizer set at 0°, only the p-polarized light passes through the polarizer. To handle this effect easily, we denote it as a linear system:

$$\begin{bmatrix} 1 \\ 0 \end{bmatrix} = \begin{bmatrix} 1 & \\ & 0 \end{bmatrix} \begin{bmatrix} 1 \\ 1 \end{bmatrix}, \tag{1}$$

where the input light, which is a mixture of p- and s-polarized light, is denoted by a vector $[1,1]^{\mathrm{T}}$ in which each element represents the intensity of the p-polarized (0°) and s-polarized (90°) components, respectively. The light then enters into the linear polarizer denoted by a 2-by-2 matrix where only the top left element is 1. As a result, the output light becomes $[1,0]^{\mathrm{T}}$, which is the p-polarized component of the light passes through while the s-polarized component is filtered out.

When the polarizer is rotated 90° (Figure 3, left middle), only the s-polarized light can pass through and the p-polarized component is filtered out:

$$\begin{bmatrix} 0 \\ 1 \end{bmatrix} = \begin{bmatrix} 0 & \\ & 1 \end{bmatrix} \begin{bmatrix} 1 \\ 1 \end{bmatrix}. \tag{2}$$

When the angle of the polarizer is set to 45°, however, we obtain 45°-polarized light as the output:

$$\begin{bmatrix} 1/\sqrt{2} \\ 1/\sqrt{2} \end{bmatrix} = \begin{bmatrix} 1/\sqrt{2} & \\ & 1/\sqrt{2} \end{bmatrix} \begin{bmatrix} 1 \\ 1 \end{bmatrix}. \tag{3}$$

We now further explain birefringence [16]. Birefringence is an optical property of a material whereby its refractive index is dependent on the polarization and direction of incoming light. Examples of such materials are calcite crystals and liquid crystals. Some birefringence materials, including LCs, have two refractive indices that correspond to incoming rays polarized either perpendicular or parallel to the optical axis of the material. The former ray is called an ordinary ray, and the refractive index is denoted by n_{or}, while the other ray is called an extraordinary ray and has a refractive index n_{ex}. As a result, the two rays are phase shifted (delay or retardation) by $2(n_{\mathrm{ex}} - n_{\mathrm{or}})\pi d/\lambda$.

Some LC panels, including PSLMs, can control this birefringence (i.e., $n_{\mathrm{ex}} - n_{\mathrm{or}}$), which is called electrically controlled birefringence (ECB).

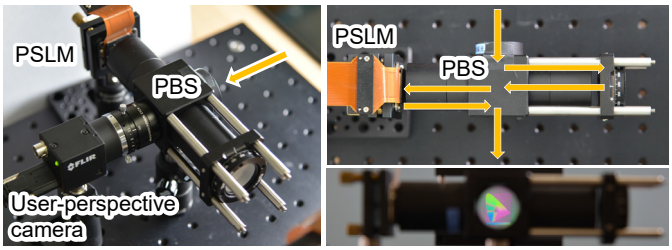

Fig. 4. A proof-of-concept system. (Left) An overview of the actual prototype. (Top right) The optical path of incoming scene light and the optical components in the system. (Bottom right) User-perspective view of the system showing an example image. See Figure 5 for a diagram of the optical process.

In the following, we explain how we implement a spatial color filter with a PSLM by using the concepts described in this section.

3.2 Jones Calculus

The behavior of the polarization state of light can be modeled via a type of linear calculus called Jones calculus [25], which we also briefly introduced in the previous section.

A PSLM works as a dynamic phase retarder [12]:

$$\mathtt{S} := e^{-\mathrm{i}\phi} \begin{bmatrix} e^{-\mathrm{i}\beta} & \\ & e^{\mathrm{i}\beta} \end{bmatrix}, \tag{4}$$

where $\beta := (n_{\mathrm{ex}} - n_{\mathrm{or}})\pi d/\lambda$, $\phi := (n_{\mathrm{ex}} + n_{\mathrm{or}})\pi d/\lambda$. Here, n_{ex} and n_{or} are the extraordinary and ordinary indices of the liquid crystal material of a PSLM and d is the thickness of the LC layer. Because $e^{-\mathrm{i}\phi}$ uniformly delays all the light regardless of s or p polarization, we may ignore it in our application. From the above, we see that PSLMs modify β to control the amount of retardance.

To use a PSLM as a polarized color filer, we now assume that the orientation angle of the LC in each cell of the PSLM is rotated 45 degrees. In Jones calculus, we can rotate a Jones matrix $\mathtt{J}$ with a 2D rotation matrix

$$\mathtt{R}(\theta) := \begin{bmatrix} \cos(\theta) & \sin(\theta) \\ -\sin(\theta) & \cos(\theta) \end{bmatrix} \tag{5}$$

as $\mathtt{R}(\theta)^{\mathrm{T}}\mathtt{J}\mathtt{R}(\theta)$. With $\mathtt{S}$ and $\mathtt{R}(\pi/4)$, we get a Jones matrix for a 45-degree rotated PSLM as

$$\mathtt{S}_{45^\circ} := e^{-\mathrm{i}\phi} \begin{bmatrix} \cos(\beta) & -\mathrm{i}\sin(\beta) \\ -\mathrm{i}\sin(\beta) & \cos(\beta) \end{bmatrix}. \tag{6}$$

By coupling the PSLM with linear polarizers with angles of 0° and 90°, we obtain the system as

$$\begin{bmatrix} 0 & \\ & 1 \end{bmatrix} \mathtt{S}_{45^\circ} \begin{bmatrix} 1 & \\ & 0 \end{bmatrix}. \tag{7}$$

Given linearly polarized light as the input, the transmittance, t, of the modulated light over the wavelength λ is given by the absolute value of the output:

$$t(\lambda) := \sin^2(\beta(\lambda)). \tag{8}$$

Note that the above equation implies that each color filter could have multiple peaks over the wavelength.

4 Light Attenuation Display

Building upon the theoretical foundation of polarization and PSLMs described in the previous section, this section describes the optical design of our light attenuation display and the rendering pipeline for filtering or enhancing colors in the physical environment.

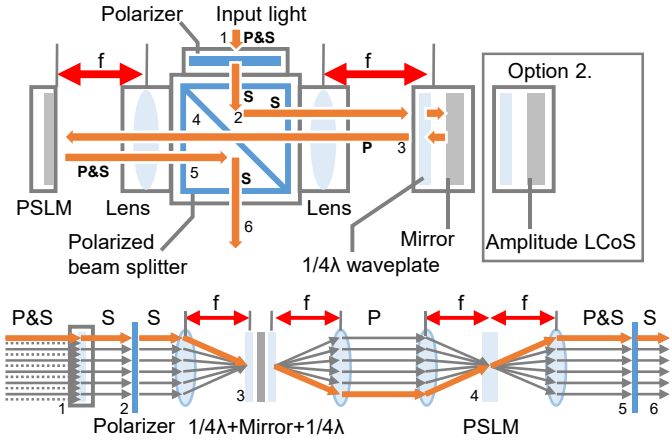

Fig. 5. Schematic diagram of the proposed system. Numbers in the diagram correspond to description in Sec. 4.1. (Top) schematic of the optics. The P and S refer to the polarization state of the input light. Placing lenses between the PBS and each reflective components, i.e. the PSLM and the mirror, is necessary to generate an image that is right side up. (Bottom) An optically equivalent setup of our system. Scene light is focused at each pixel of the PSLM. The light path is kept right side up via the dual lens design. Note that we may also replace the mirror with an ordinary amplitude LCOS, which can control the intensity of incoming polarized light. See Section 6 for further discussion.

4.1 Optical Design

Our systems has several optical requirements: (a) it must be able to integrate the color filter capability of a PSLM, which requires linearly polarized light as input, (b) it must keep the system see-through without extreme shift of the user's viewpoint, and (c) it must maintain the brightness of the see-through view (i.e., light efficiency).

Given these requirements, we implemented see-through optics with a polarized beam splitter (PBS) as shown in Fig. 4 and Fig. 5. A PBS is a cubic optical element that splits incoming unpolarized light into p-polarized and s-polarized light; the former pass through the PBS as is and the latter turns 45° and emerges from a side of the cube. In our setup, we only use the s-polarization component of the input light for a PBS by blocking the p-polarized component via an extra polarizer before the PBS. This prevents the input light from directly reaching to the viewpoint. Figure5 illustrates how the incoming light goes through the system via the color filter to the users' eye.

The path taken by the light is rather complex; for simplicity we separate it here into the six main stages (Fig. 5) from incoming light to perception of light by the user's eye (or a scene camera). First, (1) the incoming input light passes through a 0° linear polarizer, which makes the light s polarized. Once polarized, (2) the s-polarized light enters a PBS and turns 45°towards the right face of the cube. (3) The s-polarized light then passes through a quarter-wave plate and is reflected by a mirror towards the wave plate again, becoming p-polarized. Note that the tilt angle of the wave plate must be set to 45°from the normal of the s-polarized light wave to convert it from s-polarized to p-polarized. (4) The p-polarized light then passes across the PBS from right to left and hits the PSLM. Here, (5) the PSLM modulates the light which is then returned to the PBS. Finally, (6) the s-polarized component is again turned 45° and exits on the original optical axis to be perceived by the viewer or a scene camera placed at the eye's position.

Figure 5 shows a schematic diagram of the ray optics of the system with the polarization states described above. The first lens, which has a focal length of f, is necessary to focus scene light on the PSLM. Note that the current design assumes that the incoming light originates at a certain distance, typically infinite distance. Thus, the system can create sharp, pixel-wise color filters only for fixed-distance objects. The single lens design also flips the scene view upside down, requiring the placement of another lens between the mirror and the PBS.

For the PSLM, we used a Jasper Display EDK 9554 A+ (1920×1080,

60 Hz), which has a maximum retardance of about 2π at 633 nm and can be linearly controlled by 8-bit inputs. Other components were from Thorlabs: LPVISE100-A for linear polarizers, PBS251 for the PBS, WPQ10E-546 for the quarter-wave plate, BB1-E02 for the mirror, and AC254-045-A for the lenses.

4.2 Multiplexing Filter Colors in the Time Domain

Similar to many conventional displays, our light attenuation display must mix different multispectral filters to reproduce a given color. In our prototype, we employ a temporal modulation as known as field-sequential color [32], where for each pixel, we display a succession of filters which, combined, results in light that the user perceives as approximating the target color. Our algorithm first converts each observed filter spectrum into the XYZ colors by multiplying the D65 10° observer response function. We then further convert the XYZ colors into the xy colors.

Given a target RGB image and its XYZ and xy colors, we represent each target xy color by a linear combination of the filter xy colors. We first build a Delaunay diagram from the filter xy colors in the xy space. For each target xy color, we find the Delaunay triangle in which the target color lies. Because each triangle consists of three filter xy colors and the corresponding XYZ colors, we can represent the target color by a linear combination of the three XYZ colors by solving a corresponding linear equation in the XYZ space. Note that, with the current prototype, color filters do not necessarily cover the sRGB triangle; in fact some target xy colors may even sit outside the Delaunay diagram. To handle these outside points, we further apply the following heuristic algorithm.

We first take the convex hull of the original Delaunay diagram and find the edges closest to each query point lying outside the hull. After projecting an outside point onto the corresponding edge, we use the ratio of the two segments on the edge split by the projected point as the time-multiplexing ratio. Furthermore, the color filters may have different intensity levels, i.e., the norm of the XYZ color of each color filter may differ. The intensity difference propagates to the generated time-multiplexed filters. To account for the intensity issue, we weight the ratio by the Z value of the two edge points.

Once we compute the time-multiplexing ratios, we create the target color by displaying successive phase images within a specified time interval split by the ratios.

A real LCOS runs at a finite frame rate, so we must approximate continuous time-division by a set of discrete frames. Assuming that we render an image using a total of N frames for a given time-division ratio $\{r_i\}_i$, we assign each ratio round(nr_i) frames. If the sum of the frames is equal to $n+1$ or $n-1$, we search for the largest $nr_{i_{max}}$ among nr_i and decrement or increment that value.

In a real system, we need to properly determine the length of n. However, choosing the correct n has a side effect that must be considered: A smaller n deviates the generated colors from the ideal color while reducing the rendering delay. In contrast, a larger n causes the opposite effect, bringing us closer to the ideal colors but increasing the rendering delay. To investigate the effect of n, we ran a pilot rendering test.

We took an image of a color gamut and synthesized color images using the phase images generated from our algorithm with different n; the results are shown in Figure 6. For each n, we also plotted the error between the generated image and the ideal image generated from the continuous time ratios. The resulting plot is given on the left of Figure 6. As can be seen, increasing n reduces the error rapidly. After $n = 10$, the error can only be slightly improved and then only if n is significantly larger. Consequently, for the following experiments we set $n = 10$, which is also true for producing most of the results depicted in this paper, which all use field-sequential rendering.

5 Evaluation and Applications

In this section, we described experiments with our system and demonstrate some potential AR applications of the system. We first explain our measurement setup and then analyze the color filter performance of the system.

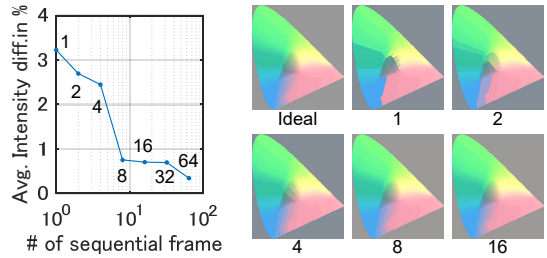

Fig. 6. Error analysis of the choice of total frame interval length. We compute output images with different frame sizes and compare them with the ideal image. (Left) Error plot. (Right) Generated images showing the produced results for each frame interval length in comparison to the ideal image.

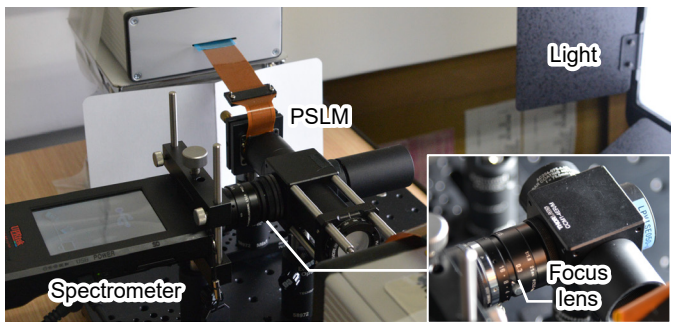

Fig. 7. Setup for measuring the spectra of the color filter output of our system. Diffuse white light with a high color rendering index (Ra≧95) is used as the light source. An object lens is attached at the exit pupil of the system so that the light passing through our filter focuses at the aperture of the spectroradiometer.

5.1 Optical Benchmark

We benchmark our proof-of-concept system in terms of its color filters.

5.1.1 Measurement Setup

The first experiment analyzes the performance of our light attenuation display with regard to the color filter properties. We place a white light source in front of the system, and we measure the spectra of the output light by using a spectroradiometer.

The light source we used, Nanguang CN-900SA, claims high color reproducibility of a color rendering index (Ra≧95). Figure 8 shows the spectrum of the light source as measured by the spectroradiometer (an UPTek MK350N Premium), which has a measurement range from 380 nm to 780 nm with a measurement step of 1 nm.

To conduct the measurement, we display uniform phase images from 0 to 255 (256 images in total) and measure the output light from each with the spectroradiometer. Before starting an actual capture, we also directly measure the light source.

Prior to taking this measurment, it is important to measure the stray light from the environment. Because the light source is located in the environment, and some random stray light passes through directly from the PBS due to the imperfection of its polarization properties, this light creates a background spectrum in the results from the spectroradiometer. Thus, after placing the spectroradiometer as shown in Fig. 7, we first take a measurement while covering the side of the PBS case that faces the PSLM. We subtract this background spectrum from each measurement.

After capturing the 256 measurements, we compute each color filter by dividing the array by the base illumination spectrum that we measured in the beginning.

5.1.2 Analysis of Measured Spectra

We next evaluate the observed color filters. The upper left image in Figure 9 is a visualization of the measured 256 color filters mapped into

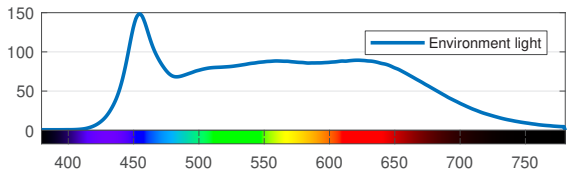

Fig. 8. The spectrum of the scene light we used for all experiments. The x-axis is the wavelength, and the y-axis is the irradiance [$\mathrm{mW/m^2}$]. The white light source has high color reproducibility in the visible spectrum.

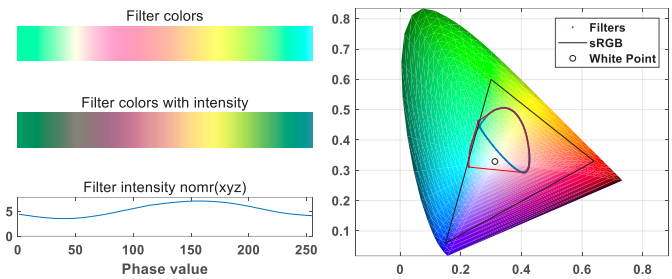

Fig. 9. Filter colors from single-phase images (top left). Filter colors over phase retardance input in the range [0,255]. The colors are reconstructed from the measured spectra using the CIE 1991 color matching function. (Middle left) In addition to the color change, we also considered the change in intensity due to the light loss of each filter. (Bottom left) Visualization of the relative intensity as the norm of the observed color filters in the XYZ color space. (right) Scatter plot (blue points) of the reconstructed colors in x-y space. The polygon around the scatter plot is a convex hull of the points. The black triangle is the sRGB range. The white circle is a D65 white point.

the RGB space. At first glance, it appears that the current prototype can create color filters dominant in red through yellow to green.

For a more qualitative evaluation of the performance, we mapped each spectrum on the xy color space via CIE XYZ 1931 standard colors (Fig. 9 bottom). In the figure, the color filters (white circles in the plot) are distributed as a smooth curve starting from a green color through a reddish color to a slightly bluish color. Taking a convex hull around the measurement shows that the color space supported by our system is currently smaller than the standard sRGB color space, which is a common color standard reproduced by conventional RGB displays.

Before exploring the spectral performance, we investigate the brightness loss of our system. To see the brightness loss, we measure the illuminance (i.e., lux) of white light input via the spectrometer with and without our see-through system. To measure the brightness of our system, we placed the light source in the same manner as the previous data collection and displayed uniform phase images with values from 0 to 255. To measure the scene light, we guided the light from the source to the spectrometer via an optical tube to block ambient light and to maintain roughly the same distance between the spectrometer and the light as in our system. We also performed an extra experiment on the brightness loss of our system. Figure 10 shows the result. Our system decreases the scene brightness from around 1,300 lux (*Environment*) to 290 lux (about 22 %, the mean of *Output brightness*). According to the WeberFechner law, the perceptual brightness sensitivity of our eyes is logarithmic [17]; thus, we may say that the perceptual brightness of our system is maintained as roughly 79 % in the $\log_{10}$ scale in this setup.

We further qualitatively assess the color filters. Figure 11 show (a) simulated color filters and (b) the observed filters of some given phase values. We calculated the simulated color filters via Eq. (8) using the retardance parameters from the actual PSLM and each Jones matrix of the optical components in our prototype. In the figure, (c) and (d) further show the color filters of the entire input phase values. As the figure shows, the simulation is a relatively good match with the observation.

Note that the retardance parameters in β of a PSLM are usually unknown and need to be measured for precise simulation [18]. In our

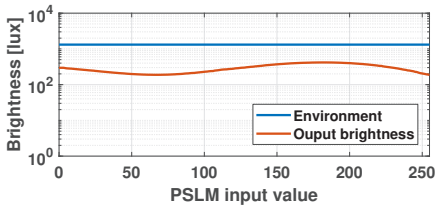

Fig. 10. Evaluation of the brightness loss of our system. We measured the direct illuminance of the scene and the illuminance of the scene as seen through the system.

simple simulation, we only knew that the PSLM is calibrated to change the phase values linearly to the designed base wavelength (633 nm). We thus manually tuned the parameters in simulation so that the simulated filters look closer to the observed filters. More concretely, we treated the unknown parameters $2(n_{\mathrm{ex}} - n_{\mathrm{or}})\pi d$ in β as a linear function of the phase input and tuned the coefficients of the function while comparing it with the observation.

Since we calibrated the system by directly measuring each resulting color filter of given phase values, the simulation only means that our derivation is valid in theory and not yet used in our applications directly.

Note that we discarded the data at the lower and higher ends of the wavelength range because the illumination used here has low intensity in those wavelength ranges, resulting in unreliable, noisy filter values.

From the spectra, we see that the color filters produced by our prototype have wide color bands and several peaks exist over the visible light band. This observation explains why the color space in the xy plot in the lower panel of Fig. 9 is relatively small, which is a drawback of the current system. One possible solution is to cascade PSLMs to improve the filter performance, as explained in the next section.

5.1.3 Dual-PSLM Setup

Given a phase shift θ, it is known that cascading phase modulation components with phase shifts proportional to the original value θ, i.e., 2θ, 3θ, and so on, makes a color filter sharper [1, 26]. To see the potential of our system with multiple PSLMs, we ran a small test of this effect using two PSLMs, with one PSLM having double the phase value of the other PSLM.

In the updated optics, we removed the mirror and replaced it with a lens, an extra quarter wave plate, and second PSLM. Fig. 12 shows the result. Compared to the single-PSLM setup (Fig. 9 and Fig. 11), the color range is expanded in green colors. In theory, our system can be stacked to further optimize the filter bandwidth, but only at the cost of the form factor and the total light intensity.

Having shown the positive result, we have to say that this simple setup is hardly optimized as there is no guarantee that doubling a phase value, i.e. 8-bit input, in a PSLM truely gives 2θ for a given wavelength. As mentioned earlier, an actual measurement of the retardance parameters of a given PSLM is necessary to optimize the design on a multiple-PSLM setup. There is also a practical problem that second PSLM requires larger phase reterdance than first PSLM.

5.2 Image Formation

Having measured the properties of the color filters, we now demonstrate the image formation using our light attenuation display. We use the same setup as described in the previous section except we replaced the spectroradiometer with a user-perspective camera (a C-mount camera (FLIR BFS-U3-32S4C-C)) with a 25 mm lens (TAMRON M118FM25). We calibrated the white balance of the camera sensor with the white light source used in the previous section. This camera configuration is used for all experiments in the remainder of this paper.

To display a target RGB image by phase input, we applied the time-multiplexing algorithm described in Sec. 4.2.

Figure 13 gives an overview of our experiment. The figure shows that our system properly renders images for given input images. Note that our display can only control chroma; it cannot control the brightness of each pixel. Thus, the resulting simulated and captured images show

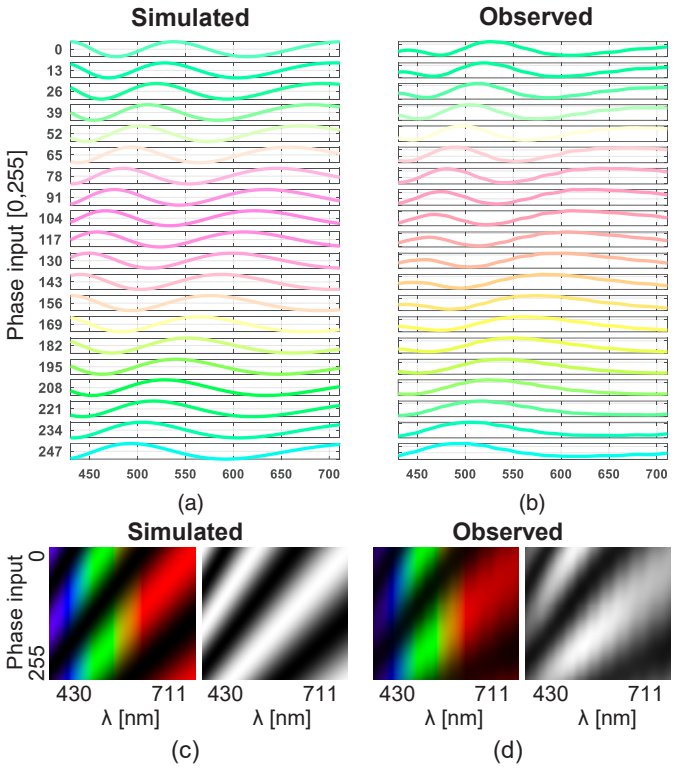

Fig. 11. Comparison between the simulated and observed color filters for the setup with a single PSLM. (a) Normalized color filter simulated using the Jones calculus in Sec. 3.2. The corresponding phase values shown are from 0 to 255 with a step size of 13. (b) Observed color filters. (c) Visualization of the color filter responses from the simulation over the entire phase values. The left image uses pseudo-colors based on the light spectrum and the right shows the filter intensity in gray. (d) Visualization of the observed color filters.

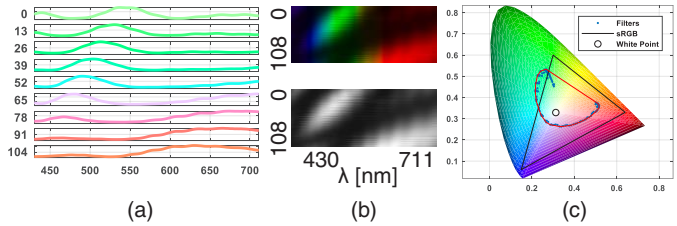

Fig. 12. Evaluation of color filters in the dual-PSLM setup. (a) Normalized, observed color filters. The corresponding phase values of the primary PSLM are from 0 to 108 with a step size of 13. (b) Visualization of the color filter responses over the phase values used. (c) Scatter plot (blue points) of the reconstructed colors of the observed color filters in x-y space. The polygon around the scatter plot is a convex hull of the points. Compared to the single setup in Fig. 9, the dual setup expanded the color range towards green outside the sRGB triangle.

degraded color. However, this is similar to additive OST-HMDs, for which the perceived brightness is constrained by the display brightness and the brightness of the environment. As mentioned before, the subtractive display will work best (e.g., produce the best contrast) in bright environments while standard additive displays produce the best contrast in dark environments.

5.3 Scene Color Enhancement and Decoloring

Apart from being able to display an image as outlined in the previous section, we see many applications for the proposed light attenuation display. Aside from traditional AR applications demonstrated later, we are also able to change the appearance of the physical environment by modulating the perceived light information via the light attenuation display. In the next experiment, we demonstrate how our light attenuation display prototype can augment the color of the see-through view of the real world. Our system can modulate the color of the scene viewed by the user by programming the color filter on a per pixel basis.

To demonstrate the system's capability, we implemented a conceptual color control application (Fig. 14). We placed a physical color chart (a ColorChecker Classic from X-Rite) in front of the system. We then computed two color filters: one replicates the color chart pattern (we call this the *enhancement setup*), and the other is a negative image of the pattern (we call this the *complement setup*). We then manually align the color filter view with the background scene and overlay the two filter images separately. Note that we used the time-multiplexing approach for phase image computation, as outlined in the previous section.

Figure 14 gives an overview of the observed results of this experiment. As expected, the resulting images of the color chart perceived by the user in the enhancement setup are more vivid, whereas the complement setup makes it less vivid.

To quantitatively analyze these color filter effects, we computed the vividness of the captured images by computing the saturation values of each image in the HSV color space (Fig. 15 right). We also want to capture a baseline view when the color filter is *off*. However, we must note that our color filters do not include the whitepoint, which means we cannot display a *colorless* color filter without time-multiplexing.

The histograms in Fig. 15 show that the enhancement setup has more points that larger saturation values compared to the histogram of the base image. On the other hand, the complement setup generally shifts the histogram towards zero, reducing the color vividness in comparison to the base image. Note that several colors on the chart or their complementary colors are far from available phase colors, which caused some artifacts in the observations. For example, the (3,4) color (yellow) in the complement setup failed to reduce vividness while maintaining the hue since it appears dark green rather than dark yellow.

Overall, this experiment successfully demonstrates that our system is capable of modifying colors in the user's view for the majority of available colors. In some rare cases, existing colors cannot be enhanced or neutralized due to some limitations in the color space.

5.4 AR Rendering

One of the most promising applications of OST-HMDs is AR. We think this is equally true for our subtractive light attenuation display. However, unlike existing OST-HMDs, the brightness of our display relies on the background illumination, i.e., the brightness of the environment. We developed some examples to demonstrate the AR capabilities of our concept, which are shown in Fig. 16. We argue that the need for a bright environment leads to several interesting application areas. First, our display prototype performs best where traditional displays have difficulty, such as outdoor environments and well-lit indoor environments. We also point out that the combination of both additive and subtractive techniques is challenging but has high potential. Investigating such a combination is clearly beyond the scope of this paper and requires a different optical design. Finally, it is worth mentioning that our light attenuation display concept does not need a back-light which is typically the main consumer of power in displays; this opens the possibility to drastically reduce the power consumption of AR devices considering only the display.

5.5 Color Compensation for AR Rendering

One common issue of typical additive OST-HMDs is that they suffer from the side-effects of optically blending the displayed color with the background. The main issue here is that the background is always part of the final result and is thus always visible. This is often undesirable, as, for example, solid objects become transparent and the visual quality is affected. The extent of this problem is typically dependent on the parameters of the optical combiner. Recently, some research has presented approaches that compensate for this effect by considering the background color captured with a camera and optimizing the displayed image for each pixel depending on the background color [23].

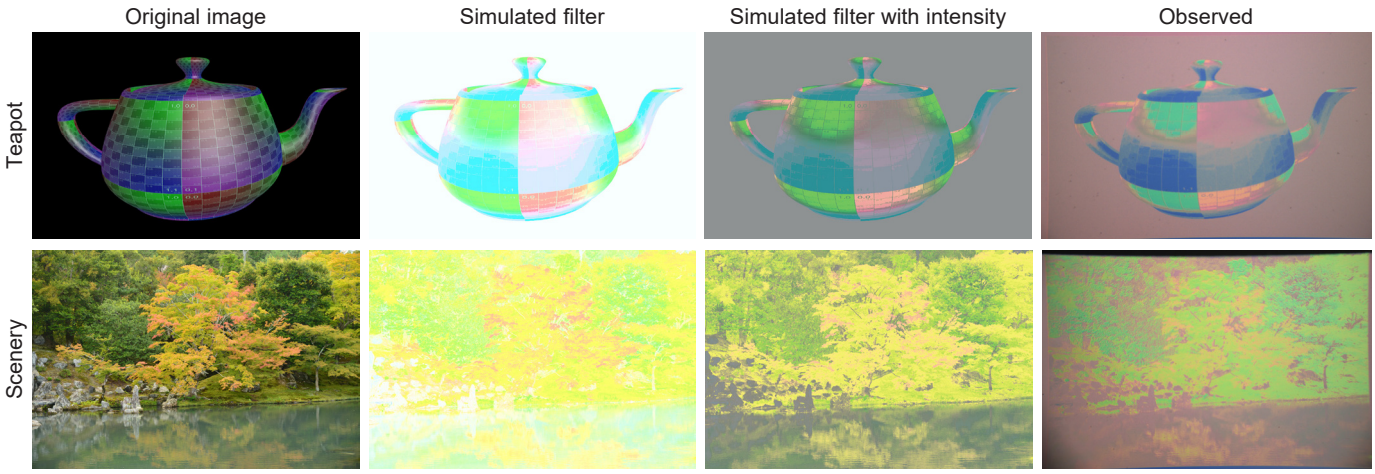

Fig. 13. Formation of images by the system with a white light source using a naive base-color mapping approach. From the left column to the right column: the original input images, the simulated filter image with uniform color intensity, the simulated color images with filter intensity, and the observed images. Although the contrast of the perceived images is degraded due to some stray light, the simulated color images are generally well reproduced. Note that the limited color chroma of the single-PSLM setup degenerates the color space of the original images. We set the phase-image frame division to 10 for each sample.

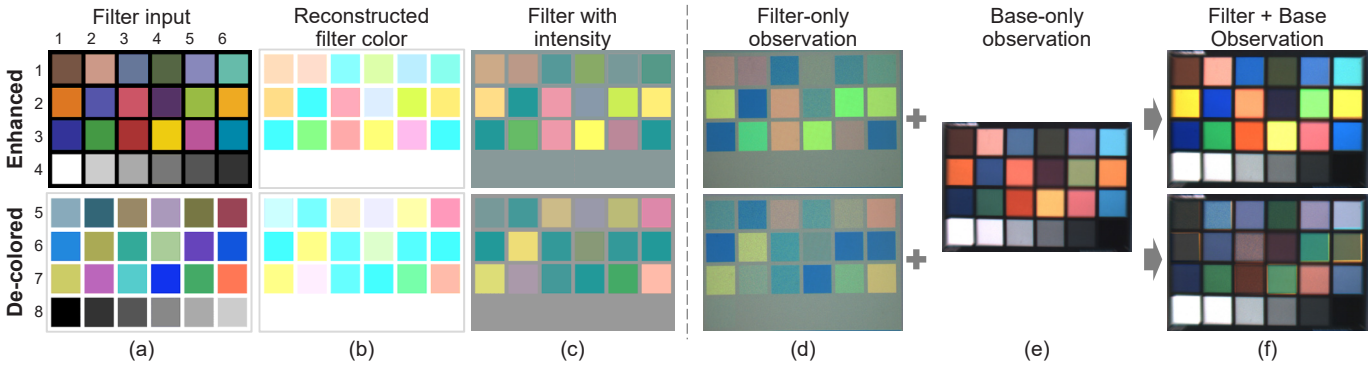

Fig. 14. Overview of results from the scene color enhancement and color diminishment or de-coloring. We display color filters that either enhance or diminish the colors of the real view. (a) The ideal filter colors. (b) Color filters simulated without considering the intensity loss. (c) With the intensity loss. (d) Real filter images displayed with white background. (e) A real color chart captured by the viewpoint camera without the color-filter effects. (f) Final observations of the scene with the two color filters aligned to the chart.

While our light attenuation display does not blend but rather filters the environment light, we are also dependent on the colors in the environment. Figure 17 shows an extreme case of different target colors over a complex scene, as seen through our light attenuation display prototype. When the naive filter that is computed without considering the background is used, the resulting image is disturbed by the background scene. Thus, we explored ways to compensate for the background, analogous to additive OST-HMDs.

For an additive OST-HMD, ignoring the optics within the HMD, the blending can be simplified as [23]:

$$R = (EM) + IF \tag{9}$$

This equation R is the blended light as perceived by the user of the OST-HMD. The incoming environment light EM is based on the environmental light source E and the material properties M of objects in the users view, which is treated singularly as environment light entering the OSTHMD. Similarly, the intensity I is the intensity of the displayed image while the form factor F describes nonlinear effects of the display (e.g., vignetting).

Given the subtractive character of our light attenuation display, the result using our display is

$$R = (EM) - I \tag{10}$$

Here I is not the displayed intensity but the filter intensity describing the actual filter. So far, we have assumed that EM is 1, but using this equation, we could also reformulate a filter I that is dependent on the environmental light EM:

$$I = (EM) - R \tag{11}$$

As well as showing an example of a non-corrected extreme case, Fig. 17 shows a corrected image based on a filter that considers the background scene color. As we can see, the resulting compensated filters contain some information from the background so that they balance the filter colors to counter the overlapping background. For example, the top row in Fig. 17 aims to render a monotone image over a multi-colored pastel background. Without compensation, the mixed view shows the filter with the background pastel colors. The compensation filter derived from the above equation gives complementary colors and the new mixed view shows a filtered image with less interference from the background, but at the cost of the filtered brightness, i.e., the image contrast. The artifacts in the image are from the LCD screen used to display the scene (background) and not from our light attenuation display prototype.

6 Discussion and Future Work

In this section, we discuss limitations of the current prototype and possible directions for future work.

Optimization of the Optics Design The current prototype serves as a general implementation of the concept and exposes several avenues for improvement. For example, the PBS limits the FoV of the

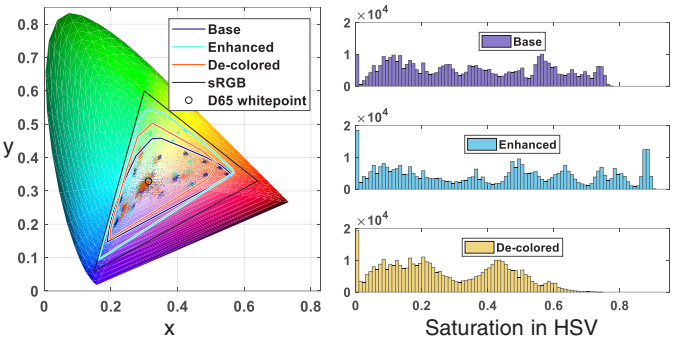

Fig. 15. Evaluation of color control. (Left) A CIE xy plot containing the observed points. The hulls are convex hulls of the points of each image. (Right) Histograms of the saturation values, i.e. the vividness, of each captured image. From the histograms, we can qualitatively see that the color enhancement filter enhances the vividness of the base image whereas the color compliment filter diminishes colors towards grey.

Fig. 16. Prototypical AR scenarios realized with our light attenuation display. Note that our prototype does not currently integrate tracking. (Left) A virtual teapot is rendered by the subtractive method onto a real scene. (Middle) A virtual text is rendered over an LED light stand. (Right) A virtual teapot is rendered over the same light source. Our system creates bright AR images even against strong background light.

system and, more crucially, prevents miniaturizing the form factor of the entire system. This design limitation inevitably stems from the use of a reflective PSLM display. One possible solution is to replace the reflective PSLM with a transmissive PSLM. However, transmissive PSLMs might introduce other problems, such as diffraction due to the pixel grid or loss of light efficiency. The different optical design enforced by a transmissive PSLM would also require extra optics to render the color filter sharp as the human eye cannot focus objects just in front of it.

The PBS design results in another issue: although our system is see-through and the view is aligned with the primary viewing axis, our system still induces a slight offset in the depth direction.

In practice, a compact, stereo glass design is desirable. To miniaturize the optics, a realistic option is to implement a polarizer on a waveguide, e.g., by using nanoimprinting [14, 37]. For instance, it might be possible to combine two such waveguide plates with a refractive PSLM to guide the incoming scene light to the PSLM through a waveguide facing the scene and then guide the output light to the eye through a second waveguide.

Amplitude Modulation Another limitation of the current light attenuation display prototype is that it only modulates chroma and not the amplitude of each filter color. One possible solution might be to combine another spatial light modulator tuned for amplitude modulation, as shown in Fig. 5. This would allow further improvement of the quality of the images generated using our prototype.

Filter Image Computation As we discussed in Sec. 4.2, we apply field-sequential color generation by displaying successive filters to create a target color. Apparently this approach reduces the temporal resolution of the display and could cause visual flickering. One solution is to use SLMs that can drive a faster than normal frame rate. Some reflective LCOS for microdisplays, for example, run at 540 Hz for sequential color rendering (e.g., ferroelectric LCDs from Citizen Fine Device Co. Ltd.). Another option might be to construct filter Bayer

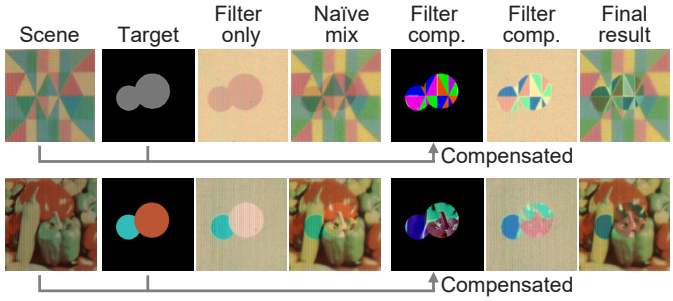

Fig. 17. Two simple examples of applying color compensation for AR rendering with an attenuation display. Note that the grid artifacts are from the image being displayed on an LCD screen and are not cause by our display prototype.

patterns to spatially assign different filter colors. This option is available at the cost of spatial resolution of the display.

Another important issue is how to accurately estimate the retardance parameters of a given PSLM [18]. Because getting such parameters enables us to reduce the calibration time of the system and, more importantly, brings options to optimize color filters for potential multiple-PSLM setups.

Color Calibration Artifacts Images may also contain possible color artifacts due to differences in the length of the optical paths from the eye to each pixel of the PSLM. This perturbs the filter property of each pixel, which might require pixel-wise color calibration for more accurate color matching, which has not been implemented in the current prototype.

Eye Tracking Requirement Along with the color artifact issue, our current system may suffer from color distribution change of the filter depending on the viewpoint of the user. In such cases, we must track the eye position and calibrate the color filter for each viewpoint accordingly. Since eye-tracking is becoming more essential for OST-HMDs, this additional hardware requirement might not be too specific.

Pixel-Level Filter for Color Blindness As shown in Sec. 5, our system can work as a spatial color filter. Thus, one direction for future applications is direct use for visual assistance, for instance, for color-vision deficiency (CVD). Recently, industry and research have presented new approaches targeting CVD, including filter-based glasses such as EnChroma [8] as well as computational glasses utilizing OST-HMDs [24]. The general idea of the former is to apply a color shift to the entire user view, while the latter system would shift critical colors in the user's view on a per-pixel level towards colors that can be perceived by the wearer. However, existing systems are limited in that they can only add extra light intensity, which can lead to unwanted color shifts and unnatural color perception.

Instead, our approach has the potential to combine both approaches by offering a per-pixel-level filter to compensate for the effect of CVD. Instead of shifting colors using the head-mounted display, our subtractive see-through head-mounted display can filter out critical wavelengths in the visible light but only for areas essential to users affected by CVD. This maintains the appearance of areas that are less affected by their CVD.

Controllable Camera Filter We also see a possible application of our approach beyond head-mounted displays. Here, we think that in particular imaging applications such as smart camera filters are a promising application area. Usually, photographers use optical filters such as neutral-density (ND) filters and graded ND filters to create unique effects in their final photos. Recently, black and white photography has also seen a comeback in the domain of digital photography. Here, optical filters (e.g., deep red filters) are usually used to improve the contrast within the final photo. The issue is that the filters are generally static and not on a per-pixel level. Our approach, however, has the potential to allow filtering of different frequencies on a per-pixel

level that can be interactively controlled without removing or changing the actual filter.

Multispectral Imaging Another application for imaging application is multispectral imaging. In conventional RGB cameras, each RGB color is assigned to different pixel, known as a Bayer filter [5]. Multispectral cameras use a rotating wheel or static prisms to capture multi-band images. Our light attenuation display may also be considered such a color filter by displaying specific phase patterns.

7 Conclusion

In this work, we presented a light attenuation display, a new type of optical see-through near-eye display that forms images through the subtraction of light from the background scene. The formation of images in our system is complementary to the additive methods used by conventional OST-HMDs, which insert extra light into the user's field of view. We implemented a proof-of-concept prototype using a phase-only spatial light modulator, which is a liquid crystal device that can control the phase of the light in each pixel. By combining PSLMs with polarization optics, our see-through system functions as a spatially programmable multispectral color filter. We evaluated the capability of the system as a display and demonstrated its potential for both an AR application and color-modulation glasses. The complementary features of our attenuation display could be powerful tools when combined with common additive OST-HMD designs.

Acknowledgments

This work was partially supported by JSPS KAKENHI Grant NumbersJP17H04692 and JP17K19985, Japan; and by JST PRESTO Grant Number JPMJPR17J2, Japan. Tobias Langlotz is partially supported by Callaghan Innovation, host of the Science for Technological Innovation National Science Challenge, Seed Project 52421, New Zealand. We also thank Prof. Masahiro Yamaguchi for sharing his expertise on optical imaging and polarization interference.

References

[1] O. Aharon and I. Abdulhalim. Liquid crystal lyot tunable filter with extended free spectral range. *Optics Express*, 17(14):11426–11433, 2009.
[2] B. E. Bayer. Color imaging array. *US patent 3,971,065*, 1976.
[3] O. Cakmakci, Y. Ha, and J. P. Rolland. A compact optical see-through head-worn display with occlusion support. In *3rd IEEE/ACM ISMAR*, pages 16–25. IEEE, 2004.
[4] M. P. Chrisp. Convex diffraction grating imaging spectrometer, Mar. 9 1999. US Patent 5,880,834.
[5] K.-H. Chung and Y.-H. Chan. A lossless compression scheme for bayer color filter array images. *IEEE Transactions on Image Processing*, 17(2):134–144, 2008.
[6] H. Dai, K. X. Y. Liu, X. Wang, and J. Liu. Characteristics of lcos phase-only spatial light modulator and its applications. *Optics Communications*, 238(4-6):269–276, 2004.
[7] G. Damberg, J. Gregson, and W. Heidrich. High brightness hdr projection using dynamic freeform lensing. *ACM TOG*, 35(3):24, 2016.
[8] EnChroma. Enchroma - see the difference.
[9] H. Fuchs, M. A. Livingston, R. Raskar, K. Keller, J. R. Crawford, P. Rademacher, S. H. Drake, A. A. Meyer, et al. Augmented reality visualization for laparoscopic surgery. In *International Conference on Medical Image Computing and Computer-Assisted Intervention*, pages 934–943. Springer, 1998.
[10] C. Gao, Y. Lin, and H. Hua. Occlusion capable optical see-through head-mounted display using freeform optics. In *11th IEEE ISMAR*, pages 281–282. IEEE, 2012.
[11] C. Gao, Y. Lin, and H. Hua. Optical see-through head-mounted display with occlusion capability. In *Proc. SPIE*, volume 8735, pages 87350F–1:9, 2013.
[12] D. Glasner, T. Zickler, and A. Levin. A reflectance display. *ACM TOG*, 33(4):61, 2014.
[13] A. Grundhöfer and D. Iwai. Recent advances in projection mapping algorithms, hardware and applications. In *Computer Graphics Forum*, volume 37, pages 653–675. Wiley Online Library, 2018.
[14] L. J. Guo. Recent progress in nanoimprint technology and its applications. *Journal of Physics D: Applied Physics*, 37(11):R123, 2004.
[15] W. Harm, A. Jesacher, G. Thalhammer, S. Bernet, and M. Ritsch-Marte. How to use a phase-only spatial light modulator as a color display. *Optics letters*, 40(4):581–584, 2015.
[16] E. Hecht. *Optics*. Pearson Education, 2016.
[17] S. Hecht. The visual discrimination of intensity and the weber-fechner law. *The Journal of General Physiology*, 7(2):235–267, 1924.
[18] A. Hermerschmidt, S. Quiram, F. Kallmeyer, and H. J. Eichler. Determination of the jones matrix of an lc cell and derivation of the physical parameters of the lc molecules. In *Liquid Crystals and Applications in Optics*, volume 6587, page 65871B. International Society for Optics and Photonics, 2007.
[19] Y. Itoh, T. Hamasaki, and M. Sugimoto. Occlusion leak compensation for optical see-through displays using a single-layer transmissive spatial light modulator. *IEEE TVCG*, 23(11):2463–2473, 2017.
[20] K. Kiyokawa, M. Billinghurst, B. Campbell, and E. Woods. An occlusion-capable optical see-through head mount display for supporting co-located collaboration. In *2nd IEEE/ACM ISMAR*, page 133. IEEE Computer Society, 2003.
[21] K. Kiyokawa, Y. Kurata, and H. Ohno. An optical see-through display for mutual occlusion with a real-time stereovision system. *Computers & Graphics*, 25(5):765–779, 2001.
[22] T. Kozacki and M. Chlipala. Color holographic display with white light led source and single phase only slm. *Optics Express*, 24(3):2189–2199, 2016.
[23] T. Langlotz, M. Cook, and H. Regenbrecht. Real-time radiometric compensation for optical see-through head-mounted displays. *IEEE TVCG*, 22(11):2385–2394, 2016.
[24] T. Langlotz, J. Sutton, S. Zollmann, Y. Itoh, and H. Regenbrecht. Chromaglasses: Computational glasses for compensating colour blindness. In *CHI*, CHI '18, pages 390:1–390:12, New York, NY, USA, 2018. ACM.
[25] G. Lazarev, A. Hermerschmidt, S. Krüger, and S. Osten. Lcos spatial light modulators: trends and applications. *Optical Imaging and Metrology: Advanced Technologies*, pages 1–29, 2012.
[26] B. Lyot. Optical apparatus with wide field using interference of polarized light. *CR Acad. Sci.(Paris)*, 197(1593), 1933.
[27] A. Maimone and H. Fuchs. Computational augmented reality eyeglasses. In *12th IEEE ISMAR*, pages 29–38. IEEE, 2013.
[28] A. Maimone, A. Georgiou, and J. S. Kollin. Holographic near-eye displays for virtual and augmented reality. *ACM TOG*, 36(4):85, 2017.
[29] A. Manakov, J. Restrepo, O. Klehm, R. Hegedus, E. Eisemann, H.-P. Seidel, and I. Ihrke. A reconfigurable camera add-on for high dynamic range, multispectral, polarization, and light-field imaging. *ACM TOG*, 32(4):47–1, 2013.
[30] N. Matsuda, A. Fix, and D. Lanman. Focal surface displays. *ACM TOG*, 36(4):86, 2017.
[31] D. L. Post, S. R. Dodd, W. C. Heinze, and R. O. Shaffner. Improved lamp and polarizers for subtractive color displays. *Journal of the Society for Information Display*, 5(3):251–259, 1997.
[32] R. G. Stewart and W. R. Roach. Field-sequential display system utilizing a backlit lcd pixel array and method for forming an image, Aug. 9 1994. US Patent 5,337,068.
[33] I. E. Sutherland. A head-mounted three dimensional display. *Fall Joint Computer Conference*, pages 757–764, 1968.
[34] B. Thomas, B. Close, J. Donoghue, J. Squires, P. De Bondi, and W. Piekarski. First person indoor/outdoor augmented reality application: Arquake. *Personal and Ubiquitous Computing*, 6(1):75–86, 2002.
[35] T.-H. Tsai, X. Yuan, and D. J. Brady. Spatial light modulator based color polarization imaging. *Optics Express*, 23(9):11912–11926, 2015.
[36] C. Wang, Q. Fu, X. Dun, and W. Heidrich. Megapixel adaptive optics: towards correcting large-scale distortions in computational cameras. *ACM TOG*, 37(4):115, 2018.
[37] J. Wang, S. Schablitsky, Z. Yu, W. Wu, and S. Y. Chou. Fabrication of a new broadband waveguide polarizer with a double-layer 190 nm period metal-gratings using nanoimprint lithography. *Journal of Vacuum Science & Technology B*, 17(6):2957–2960, 1999.
[38] G. Wetzstein, W. Heidrich, and D. Luebke. Optical image processing using light modulation displays. In *Computer Graphics Forum*, volume 29, pages 1934–1944. Wiley Online Library, 2010.
[39] Y. Yamaguchi and Y. Takaki. See-through integral imaging display with background occlusion capability. *Applied Optics*, 55(3):A144–A149, 2016.
[40] Z. Zhang, Z. You, and D. Chu. Fundamentals of phase-only liquid crystal on silicon (lcos) devices. *Light: Science & Applications*, 3(10):e213, 2014.